

What is the potential for a second peak in the evolution of SARS-CoV-2 in Brazil? Insights from a SIRASD model considering the informal economy

M. A. Pires^a, N. Crokidakis^b, D. O. Cajueiro^{c,d,e}, M. Argollo de Menezes^{b,c}, S. M. Duarte Queirós^{a,c}

^a*Centro Brasileiro de Pesquisas Físicas, Rio de Janeiro/RJ, Brazil*

^b*Instituto de Física, Universidade Federal Fluminense, Niterói/RJ, Brazil*

^c*Instituto Nacional de Ciência e Tecnologia de Sistemas Complexos INCT-SC, Rio de Janeiro/RJ, Brazil*

^d*Departamento de Economia, Universidade de Brasília, Brasília/DF, Brazil*

^e*Machine Learning Laboratory for Finance and Organizations, Universidade de Brasília/DF, Brazil*

Abstract

We investigate the emerging scenarios from a two-population Susceptible-Infected-Recovered-Asymptomatic-Symptomatic-Dead (SIRASD) model, where populations differ by their degree of compliance with social distancing policies. Considering the data of the propagation of SARS-CoV-2 in Brazil, where there is a significant stake of the population making their living in the informal economy and thus prone to not follow self-isolation, we assert that if the confinement measures are lifted too soon, namely as much as one week of consecutive declining numbers of new cases, it is very likely the appearance of a second peak .

Keywords: Collective phenomena, Multi-group epidemic models, Peak Analysis

Contents

1	Introduction	1
2	Model	3
3	Results	4
4	Discussion	9
5	Limitations	10
6	Final remarks	10

1. Introduction

The ongoing COVID-19 pandemic has turned into the deepest global health crisis of our time. It started in China and has already spread across the five continents. Although there are some differences among the countries public health policies, the vast majority of them has tried to reduce the growth rate of the pandemic by implementing policies of social distancing [1] aiming at preventing mayhem of the health-care systems, the so-called “flattening of the curve”. A series of models have been brought forth to the specific study of the evolution of COVID-19 through the world [2, 3, 4, 5, 6, 7, 8, 9, 10, 11, 12, 13, 14, 15, 16, 17, 18, 19, 20, 21, 22, 23, 24, 25, 26, 27, 28,

Email address: nuno@mail.if.uff.br (Corresponding author) (N. Crokidakis)

29, 30, 31]. Initially, some of those works focused on its calibration in order to estimate typical parameters of the disease, like infection rates, epidemic doubling times among others [3, 5, 16, 17, 18, 19, 22, 23, 26, 27, 28]. After these preliminary studies, many authors considered the effect of several types of non-pharmaceutical interventions [2, 4, 10, 11, 12, 13, 14, 15, 20, 21, 24, 25, 31].

Despite the concerns related to public health, there are other impacts due to the implementation of social isolation policies. For example, it has been reported a decrease of 4.2% in global CO_2 emission in first quarter of 2020 [32]. In addition, we also observe economic impacts due social distancing policies. Indeed, in some countries a considerable amount of the population is occupied with informal employments. These individuals, as well as people working in fundamental activities (hospitals, supermarkets, drugstores, and others) usually are not obeying the social distancing policies due to their professional activities.

A study analyzed the impacts of mobility lockdown in Italy due to the fast spreading of COVID-19 [33] in which the authors identified two ways through which mobility restrictions affect the population. They verified that the impact of lockdown is stronger in municipalities with higher fiscal capacity, and also that mobility restrictions are stronger in municipalities for which inequality is higher and where individuals have lower income per capita, causing a segregation effect. In Ref. [33] the authors also discussed about the income distribution, that play an important role: municipalities where inequality is greater have experienced stronger increase in mobility and their citizens are more at risk. Finally, they concluded that the results suggest the necessity of asymmetric fiscal measures. In other words, according to that work, central governments should implement financial transfer mechanisms to people, companies and local local government in the form of living allowances, no-interest loans and treasury transfers to compensate the loss of tax income to allow each case to cope with the current scenario. As also stated in Ref. [33], the absence of targeted lines of intervention during the lockdown would induce a further increase in poverty and inequality.

Another work deals with wealth distributions under the spread of infectious diseases [34]. Considering the coupling of a compartmental epidemic dynamics with a kinetic model of wealth exchange, the authors found that that the spread of the disease seriously affects the distribution of wealth. Indeed, the evolution of a disease together with the dynamics of wealth exchange changes the wealth distributions from a bimodal form to a fat-tailed one [34]. Still talking about economic implications of mobility restrictions, it was reported the decline of Gross Domestic Product in China [35].

In this work, we intend to discuss the effectiveness of social distance policies in developing and emerging countries where the share of informal employment in total employment is very high. Although it is not always true that there is a relationship between informal employment and poverty, we may find a clear positive relationship among them. It is worth mentioning that in developing and emerging countries the share of informal employment in total employment ranges from 50 per cent to more than 98 per cent [36]. In this context, we investigate emerging scenarios for a generalized SIR-like model taking into account a heterogeneous propensity of individuals to comply with the self-isolation policies.

Our work relates to the recent interesting contributions that consider the effect of social factors into epidemics models [37, 38, 39, 40] and works that have tried to study and forecast the early evolution of the COVID-19 pandemics and the public policy response to it [3, 4, 6, 7, 8, 9].

The rest of the work is organized as follows: In Section 2, we introduce the SIRASD models used in this work

and how we split the population in two groups: the group of individuals that work in the informal economy can afford partially self-isolation and the rest of population that has the choice of self-isolation. In Section 3, we present the main results of our model. Furthermore, while Section 4 presents a discussion of our results, Section 5 presents their limitations. Finally, Section 6 stresses the main results of the our work.

2. Model

We divide the population into two types of individuals:

- Type 1: the group that has the option of self-isolation. This group represents a fraction f_1 of the full population.
- Type 2: low income workers in the gig economy and informal sectors. This group represents a fraction $f_2 = 1 - f_1$ of the full population.

Let ϕ_u be the noncompliance degree of the group u concerning governmental containment policies. Thus $1 - \phi_u$ is the degree of engagement with self-isolation advice.

For the COVID-19 there are both asymptomatic and symptomatic cases. Thereby we consider a framework close to [4] (and references therein). That is we consider a SIRASD (Susceptible-Infected-Recovered-Asymptomatic-Symptomatic-Dead) model where here extend it for the inclusion of two groups.

To explain in details our model consider two individuals $\{i, j\}$ belonging to the groups $\{u, z\}$, respectively. Then

- If i is in the state S and if j is infected in the state $X = \{A \text{ or } I\}$ then a transmission event occurs in which i enters in the state I with rate $p\phi_z\phi_u\beta_X$ or enters in the state A with rate $(1 - p)\phi_z\phi_u\beta_X$. Where p proportion of individuals who develop symptoms.
- If i is in the state A then it enters in the state R with rate γ_A .
- If i is in the state I then it enters in the state D with rate $q\gamma_I$, otherwise it enters in the state R with rate $(1 - q)\gamma_I$. Where q is the probability of an individual in the class I dying from infection before recovering

It is important to stress that $D(t)$ informs how many individuals who tested positive for COVID-19 were declared dead at date t .

An illustration of transition between the compartments is shown in Fig.1. From the aforementioned rules the set of coupled ODEs that governs the system considering the mean-field assumption. Explicitly, we arrive at:

$$\frac{dS_u}{dt} = -\frac{S_u}{N} \sum_{z=1}^2 \phi_u\phi_z(\beta_I I_z + \beta_A A_z), \quad (1)$$

$$\frac{dA_u}{dt} = \frac{S_u}{N} (1 - p) \sum_{z=1}^2 \phi_u\phi_z(\beta_I I_z + \beta_A A_z) - \gamma_A A_u, \quad (2)$$

$$\frac{dI_u}{dt} = \frac{S_u}{N} p \sum_{z=1}^2 \phi_u\phi_z(\beta_I I_z + \beta_A A_z) - \gamma_I I_u, \quad (3)$$

$$\frac{dR_u}{dt} = (1 - q)\gamma_I I_u + \gamma_A A_u, \quad (4)$$

$$\frac{dD_u}{dt} = q\gamma_I I_u, \quad (5)$$

with $N = \sum_{u=1}^2 (S_u + A_u + I_u + R_u + D_u)$. The interaction can involve individuals within the same group (intragroup interaction: $\phi_1\phi_1, \phi_2\phi_2$) or between different groups (intergroup interaction: $\phi_1\phi_2, \phi_2\phi_1$).

All the epidemiological parameters used in this study comes from [4]: $\beta_A = 0.458$, $\beta_I = 0.455$, $\gamma_A = 0.144$ and $p = 0.624$. To obtain q , γ_I and ϕ_u we still need to apply a term-by-term comparison between our Eqs. (1)-(5) and their system of Eqs. 4 considering a group-free population:

- $q\gamma_I \equiv \gamma_S\rho/(1-\rho)$
- $(1-q)\gamma_I \equiv \gamma_S$
- $\phi_u\phi_u = \psi$.

Thus, $q = \rho = 0.029$, $\gamma_I = \gamma_S/(1-\rho) = 0.149$ and $\phi_u = \sqrt{0.638} = 0.799$

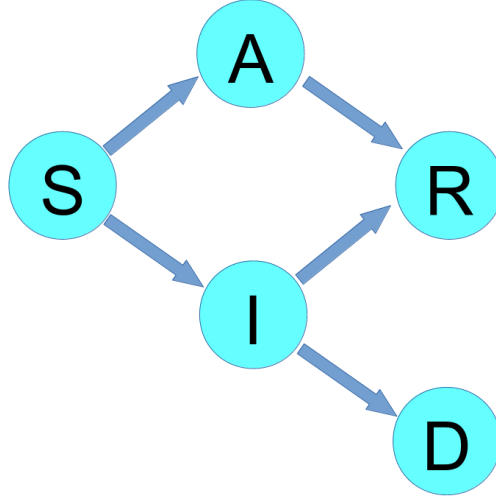


Figure 1: Susceptible-Infected-Recovered-Asymptomatic-Symptomatic-Dead (SIRASD) compartmental model.

3. Results

In this section we present the results solving our coupled ODEs using the *solveivp* of python. Specifically, we use the *RK45* method that implements an explicit Runge-Kutta method of order 5(4). Such procedure manages the error considering an accuracy of the 4-order and it employs a 5-order accurate formula to take the steps. We set $N = 210147125$. We consider an initial condition as $I_1(t_0) = 1$ and $A_1(t_0) = 0.5$ for the group 1. For the group 2 we set $I_2(t_0) = A_2(t_0) = 0$.

Apart from the number of individuals in each class, there is a second quantity of interest, namely the Relative Epidemic Size (RES) that is computed from t_0 to t

$$RES = \sum_{z=1}^2 \frac{S_z(t_0) - S_z(t)}{N} \quad (6)$$

In order to better grasp our full protocol lets first consider the case with $f_1 = 1$. Let u be the index of group u . We consider $\phi_u = \phi_u^{(0)} = 1$ during the initial stage of the epidemic spreading because the level of self-isolation is

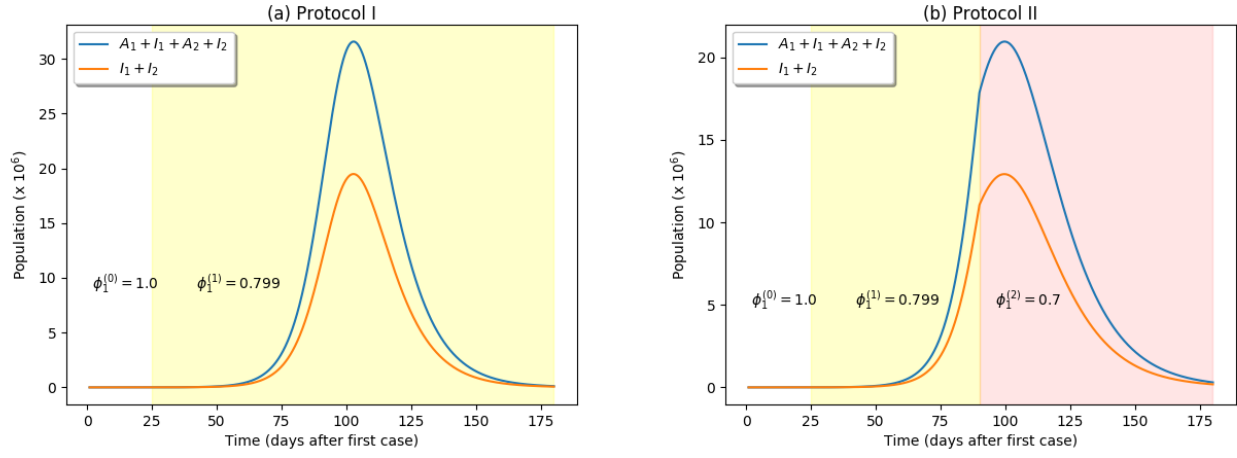


Figure 2: Time series for the number of individuals in the class $\sum_i I_i$ as well as $\sum_i (A_i + I_i)$ considering the protocols I (left) and II (right). In the protocol II we apply $\phi = 0.799 \rightarrow \phi = 0.7$ on day $t_{policy}^{(2)} = 90$ after the first case (red shaded region).

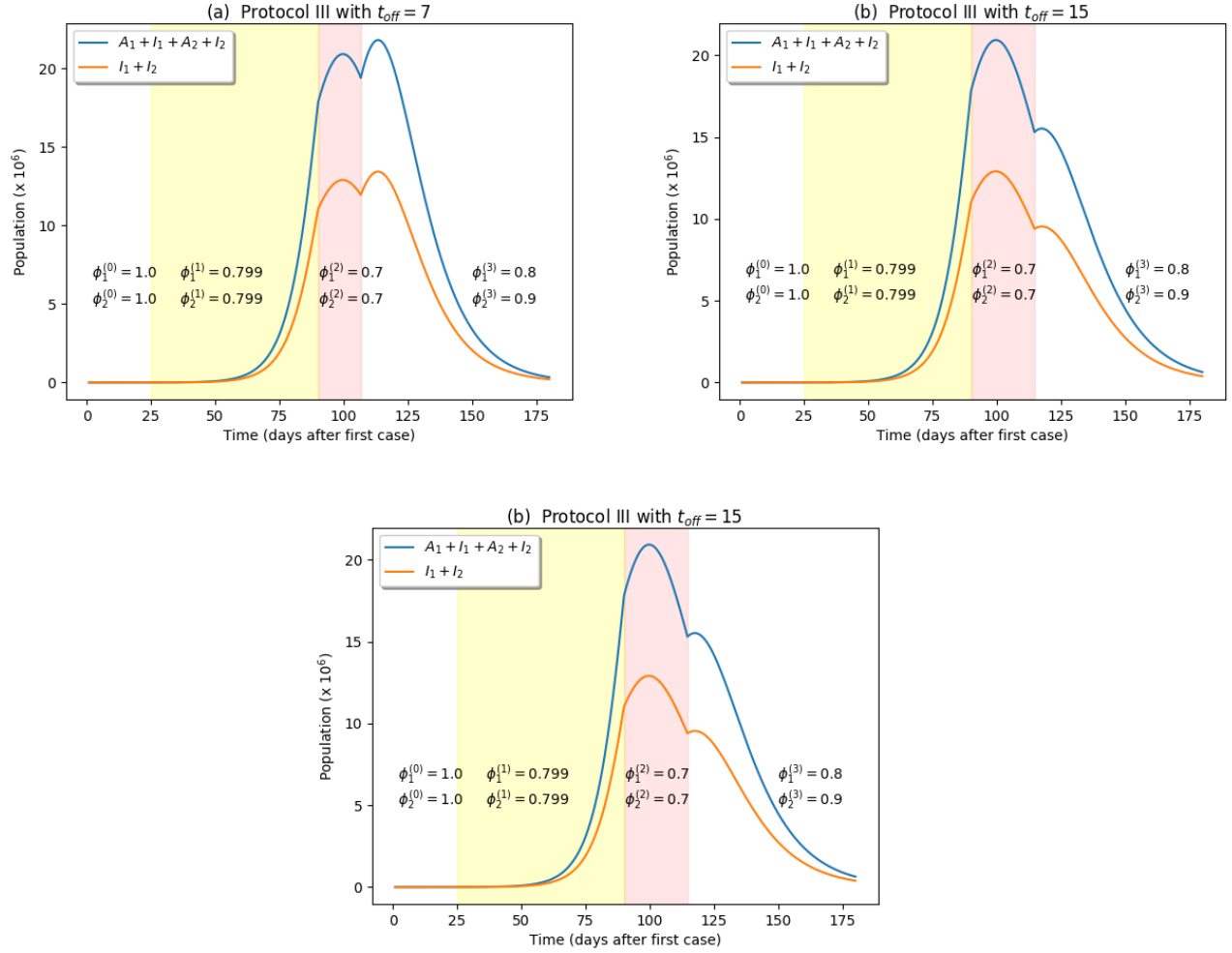


Figure 3: Time series for the number of individuals in the class $\sum_i I_i$ as well as $\sum_i (A_i + I_i)$. The first white, yellow and red shaded areas are explained in the previous Figure. The last white region represents the case with soft self-isolation rules.

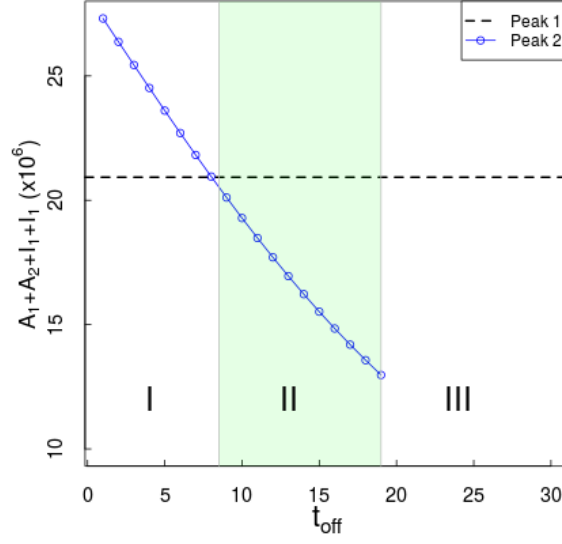


Figure 4: Dependence of the peak size of $\sum_i (A_i + I_i)$ with t_{OFF} . Parameters: $t_{\text{max}} = 365$, $f_1 = 0.6$, $\phi_1^{(2)} = \phi_2^{(2)} = 0.7$, $\phi_1^{(3)} = 0.8$ and $\phi_2^{(3)} = 0.9$. Regime I: the second peak is larger than the first one. Regime II: the secondary peak is smaller than the first one. Regime III: absence of a second peak. Each of these regimes is illustrated in Fig. 3.

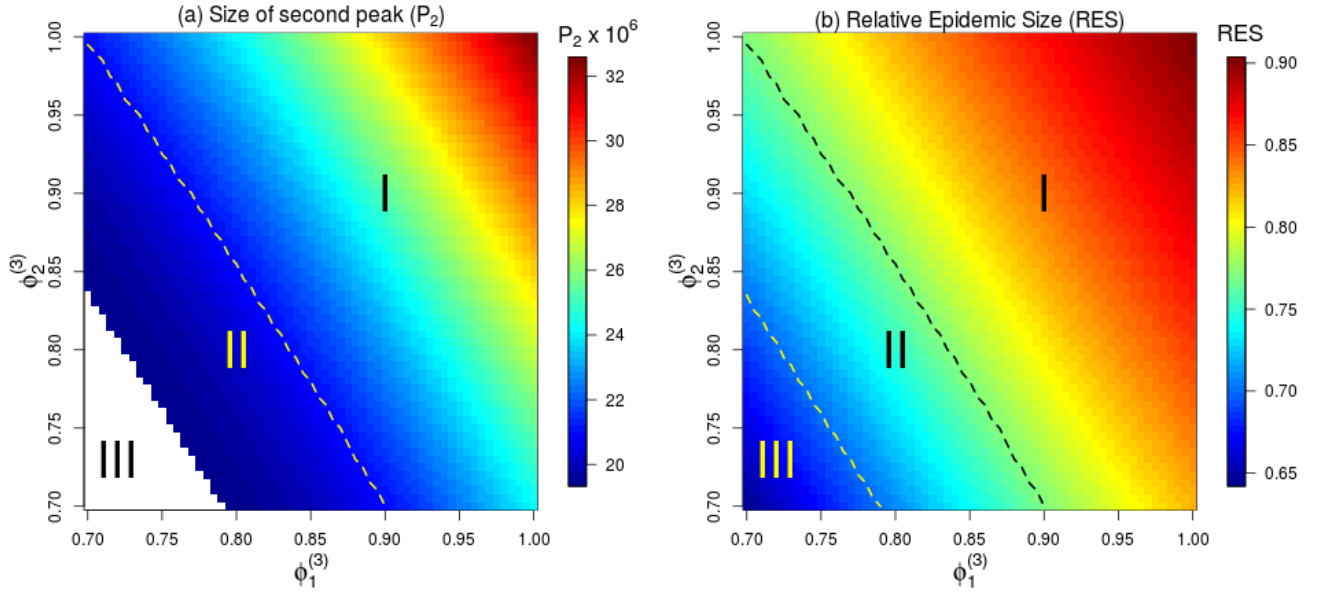


Figure 5: Dependence of P_2 as well as RES with ϕ_1^{off} vs ϕ_2^{off} . Diagrams obtained for $t_{\text{max}} = 365$ days, $t_{\text{OFF}} = 7$, $f_1 = 0.6$ and $f_2 = 0.4$. The regimes I, II and III are explained in the Fig. 4. P_2 is computed considering both symptomatic and asymptomatic individuals, ie $A_1 + A_2 + I_1 + I_2$.

almost null. We shall assume $\phi_u^{(0)} \rightarrow \phi_u^{(1)} = 0.799$ on day $t_{policy}^{(1)} = 25$ after the beginning of the epidemic spreading. With this procedure (we call it protocol I) we obtain the time series shown in Fig.2(a) that recover the results presented in [4] considering the scenarios with the current confinement rules imposed by the government for an indefinite time.

Consider the protocol II shown in Fig.2(b). During the explosive growth of the epidemic, the isolation policy is improved by better surveillance. Explicitly, we decrease the noncompliance degree from $\phi_u^{(1)} = 0.799$ to $\phi_u = \phi_u^{(2)}$ on day $t_{policy}^{(2)} = 90$ after the first case at day t_0 . Henceforth we set $\phi_u^{(2)} = 0.7$, but the nature of our results does not change qualitatively for other values. In Fig.2(b) we see that such strengthening of the confinement restrictions leads to a substantial decrease in the number of symptomatic and asymptomatic individuals.

The self-isolation measures are permanent in the protocols I and II. However, after the epidemic growing phase, there might be political and economic pressure to ease strict confinement rules. In that sense, let's us move to the protocol III with temporary self-isolation guidelines. Explicitly,

- After each time step (day) we monitor $\delta I(t) = \sum_z (I_z(t) - I_z(t-1))$
- At t_0 we set $t_{decrease} = 0$. For each $dI(t) < 0$ we increase $t_{decrease}$ in one unit.
- If $t_{decrease} = t_{OFF}$ we set $\phi_u = \phi_u^{(3)}$. That is if $dI(t) < 0$ during t_{OFF} consecutive days, the social distancing rules are relaxed.

Figure 3 exhibits the time series for the number of individuals infected considering $f_1 = 0.6$ and $f_2 = 0.4$. The self-isolation measures are lifted t_{OFF} days after the peak. At that moment the degree of the degree of noncompliance is increased to $\phi_1^{(3)} = 0.8$ and $\phi_2^{(3)} = 0.9$ (last white regions in Fig. 3). If the interruption of the confinement rules takes place one week after the peak, $t_{OFF} = 7$, we see that the second peak is worse than the first one. This scenario is different for $t_{OFF} = 15$, where the secondary peak is smaller than the first one. If $t_{OFF} = 30$ days then there is no rising of the secondary peak even though there is a rise in the person-to-person contagion.

Figure 4 shows how the time for interruption of the confinement rules impacts the epidemic spreading behavior. The peak size is computed taking into account both symptomatic and asymptomatic individuals $A_1 + A_2 + I_1 + I_2$. Specifically, there are three main outcomes. Easing the mobility restrictions too soon triggers an abrupt rise of the new cases that leads to a pronounced second peak that is worse than the first one. This is the first regime. In regime II, the secondary chain of contagion also leads to a new noticeable outbreak but now with magnitude smaller than the first one. In regime III, there is no second local maximum. Then, we highlight that there are two thresholds: (i) for prevention of a second large-scale epidemic outbreak; (ii) for prevention of a second small-scale outbreak.

Figure 5 disentangles the role played by the degree of noncompliance $\phi_u^{(3)}$ of each group u . When the confinement guidelines are lifted too early ($t_{OFF} = 7$) the majority of the combinations of $\phi_1^{(3)}$ vs $\phi_2^{(3)}$ leads to the regime I where the second outbreak is more aggressive than the first one. In this setting, the relative epidemic size (RES) can achieve about 90% of the population in the long-run (1 year in such figure). For combinations of moderated values of $\phi_1^{(3)}$ vs $\phi_2^{(3)}$, there is a substantial region in regime II where RES is mostly between 70%-80% of the population. The non-negligible presence of the regime III indicates that the prevention of a secondary epidemic outbreak can be achieved if the engagement of the population with the stay-at-home guidelines does not decrease too much.

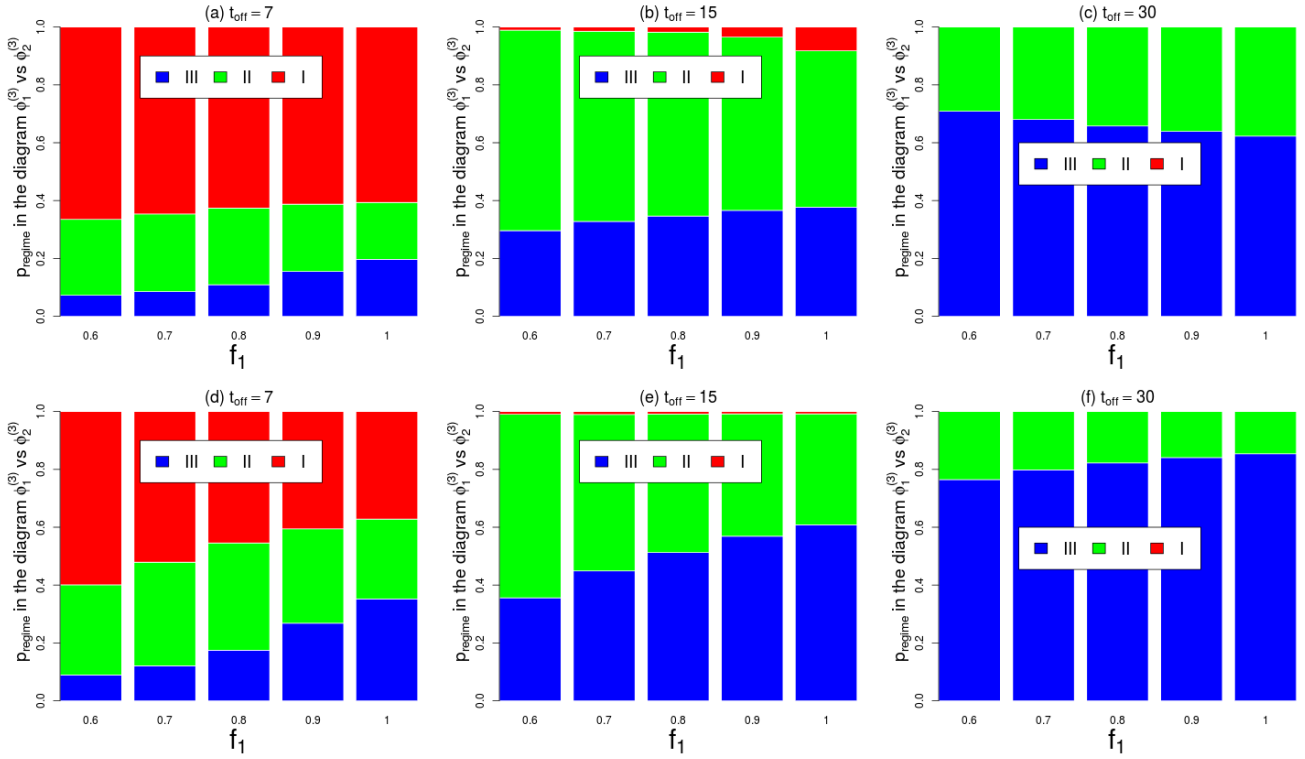


Figure 6: Barplot with the proportion of each regime p_{regime} in diagrams similar to the shown in Fig. 5. (Top) All 61×61 combinations of $\phi_1^{(3)} \times \phi_2^{(3)} \in [0.7, 1] \times [0.7, 1]$. (Bottom) Combinations satisfying $\phi_2^{(3)} \geq \phi_1^{(3)}$.

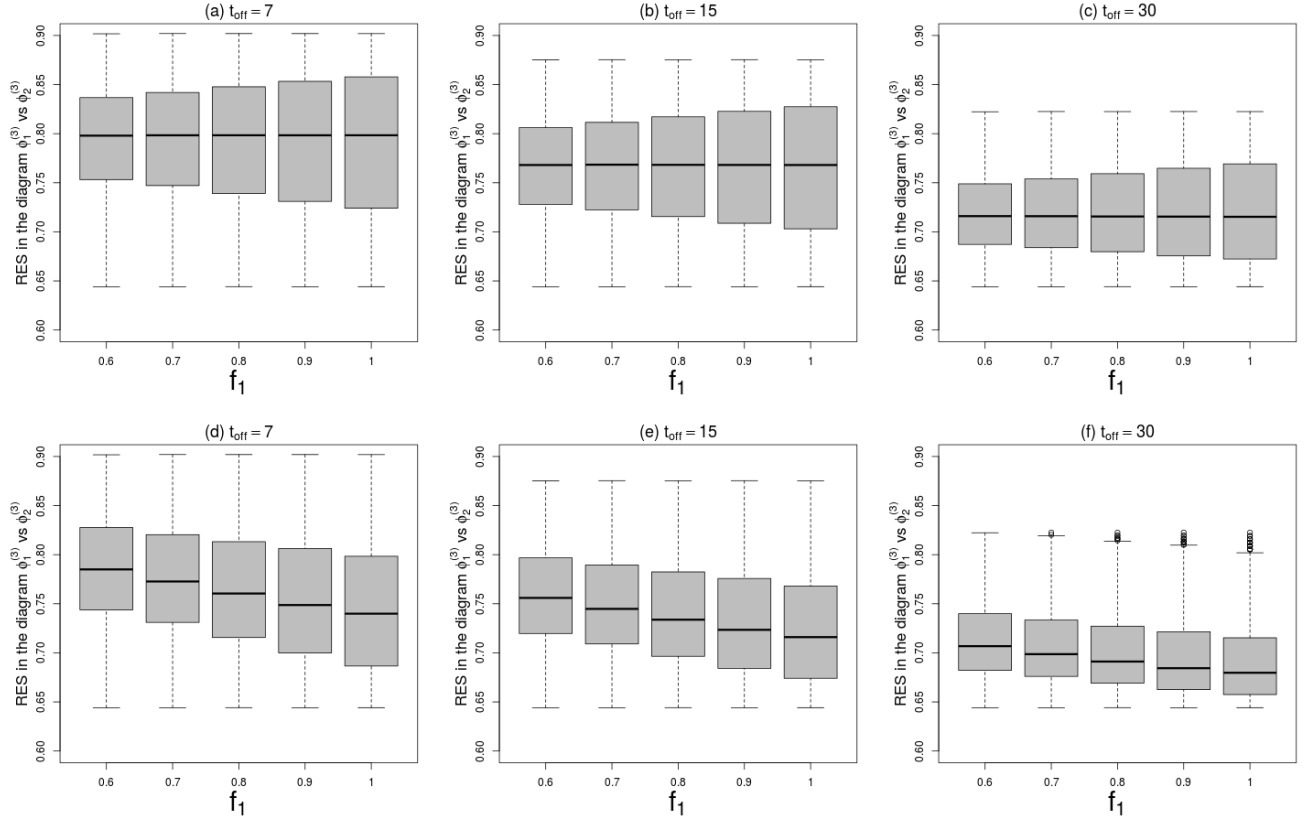


Figure 7: Boxplot with the range of values exhibited by RES in diagrams similar to the shown in Fig. 5. (Top) All 61×61 combinations of $\phi_1^{(3)} \times \phi_2^{(3)} \in [0.7, 1] \times [0.7, 1]$. (Bottom) Combinations satisfying $\phi_2^{(3)} \geq \phi_1^{(3)}$.

Let us now turn our attention to our main results depicted in Figs.6-7 for $f_1 = \{0.6, \dots, 1\}$ and $t_{\text{OFF}} = \{7, 15, 30\}$. In panels (a-c) each barplot or boxplot is obtained considering grids with 61×61 combinations of $\phi_1^{(3)} \times \phi_2^{(3)} \in [\phi_1^{(2)}, 1] \times [\phi_2^{(2)}, 1]$ where $\phi_1^{(2)} = \phi_2^{(2)} = 0.7$. Thus, all the panels (a-c) totalize $3 * 5 * 61 * 61 = 55815$ different projections. The panels (d-f) show the results for the those combinations satisfying $\phi_2^{(3)} \geq \phi_1^{(3)}$. In the boxplot the gray shaded box goes from the first quartile to the third quartile and the horizontal line inside the box is the median.

Figure 6 shows the barplots for the proportion of each regime p_{regime} for several f_1 and t_{OFF} . In the setting with $t_{\text{OFF}} = 7$ and $f_1 = 0.6$, the overwhelming majority of configurations lead to the establishment of the regime I, as previously observed. But, this advantage of the regime I decrease as f_2 decreases (by increasing f_1). In the setting with $t_{\text{OFF}} = 15$ all the scenarios exhibit a smaller proportion for the regime I in comparison with corresponding scenarios for $t_{\text{OFF}} = 7$. However, there is a dual effect of rising f_1 . On the one hand, it increases the proportion of configurations associated with the regime III. On the other hand, it also increases the possibilities for the emergence of regime I. In the setting with $t_{\text{OFF}} = 30$ we also see a double-edged sword: (a) the percentage of regime I is null and all the percentage of the regime III are higher than the corresponding to the cases $t_{\text{OFF}} = \{7, 15\}$; (b) an increase of f_1 increases the relative advantage of regime II. These nonmonotonic effects arises because some combinations $\phi_1^{(3)} \times \phi_2^{(3)}$ favor the regime I and other combinations favor the regime III as depicted in Figure 5. Such mechanism is corroborated with the panels (d-f) where we see that the combinations satisfying $\phi_2^{(3)} \geq \phi_1^{(3)}$ leads to a monotonic behavior of p_{regime} vs f_1 for all $t_{\text{OFF}} = \{7, 15, 30\}$.

Figure 7 shows the boxplots for RES considering decreasing values of $f_2 = 1 - f_1$ as well for increasing values of t_{OFF} . Such results show that an increment in t_{OFF} leads to an overall decrease in the relative epidemic size (RES). But a detailed analysis in each panel shows that an increase in f_1 produces an increase in the interquartile range of values for RES (gray area). This indicates the presence of a twofold effect since RES can achieve smaller values as f_1 increases, but it also leads to the possibility for RES reaching higher values. Again such twofold effect arises because some combinations $\phi_1^{(3)} \times \phi_2^{(3)}$ are responsive for an increase in RES and other combinations promote a decrease in RES as unveiled in Figure 5. This is confirmed with the panels (d-f) where the combinations satisfying $\phi_2^{(3)} \geq \phi_1^{(3)}$ leads to an increase in RES as f_1 where increase for all $t_{\text{OFF}} = \{7, 15, 30\}$.

4. Discussion

The findings in Figs.6-7 are our main results. Such figures show that for epidemiological parameters estimated from data of SARS-CoV-2 in Brazil it is very likely the emergence of a second peak (regimes I+II) if the preventive measures are lifted too soon. Even more alarming, there is a non-negligible risk for the magnitude of such second peak be higher than the first one (regime I). Apart from this, we note that for a given t_{OFF} there is the possibility for a twofold effect in which an intervention designed to hamper the epidemic spreading can backfire. However, in such a situation the establishment of positive or negative outcomes depends on the combinations of $\phi_1^{(3)}$ vs $\phi_2^{(3)}$ as indicated in Fig.5. Such findings highlight that it is significant to have a substantial alignment between different interventions designed to decrease the degree of noncompliance as well as to support the fraction of the population that cannot afford for the self-isolation even after the first peak of spreading. Moreover, complementary studies using different parameters to the Brazilian case we could verify that the present model is also capable of reproducing different situations of separated peaks as found in several U.S.A. cities during the spanish flu pandemics [41, 42]. Therein,

it is possible to assess the impact of different public health measures in the number and evolution of fatalities, with some cities basically exhibiting a single peak (an indicator of proper policies) and other cities with significant second peaks. Importantly, some of the cities showing two peaks were cities that had social-economical problems reminiscent of those one can find in Brazil. In other words, although we have adjusted our model to the present COVID-19 case, our model is likely to be relevant in the analysis of other situations, namely the computational forward testing of public health policies.

Other correlated works considering epidemiological parameters estimated from data of COVID-19 spreading in other countries have also shown the possibility of a second epidemic peak. In [43] it is shown – with variants of the SIR model – the potential of the second peak of infections for the UK. In [44] they calibrated a stochastic agent-based model from data in France and they projected that it would be unlikely to prevent the second chain of contagions once quarantine is lifted. A second chain of spreading was also predicted – using a generalization of the SIR model – as a potential outcome for Italy after the relaxation of the mobility restrictions [45]. A recent work considering the case of Brazil in a group-free Susceptible-Exposed-Infected-Recovered-Dead model presented some time series suggesting that the social isolation must hold until the end of 2020 in order to diminish the second peak [29]. Effectively, the conclusion of all those works is that the safer situation is to hold the isolation for as long as possible in order to decrease the second peak height.

5. Limitations

We consider that as the epidemic starts to climb sharply there will be an increased pressure to decrease the degree of noncompliance (red shaded region in Fig.3). At this point we still assumed the same level of compliance of both groups because of the current implementation of income transfer for the group 2. After the first peak and as soon as the stay-at-home restrictions are suspended we set different levels of compliance with the post-quarantine stage for each group (last white region in Fig.3).

Besides, our work does not consider explicitly an upper bound for the capacity of the healthcare system. Under-reporting is another feature that is not modeled here and we have not considered the clear regional heterogeneity in Brazil as well.

All of these constraints can induce quantitative fluctuations in the time series for the COVID-19 in Brazil, however, we do not expect qualitative discrepancies concerning our projections about the risk of a second peak of transmissions if the confinement rules are suspended too early.

6. Final remarks

Our work have used Brazilian data to model the evolution of the dynamics of COVID-19, to analyze the effectiveness of social distancing policies and to estimate the likelihood of arising a second peak in Brazil. We apply a SIRASD model considering a population split in two groups with different behaviours, namely a group that belongs to a class that is able to self-isolate and a group that is formed by low income workers in the gig economy or informal sectors. While the first group usually belongs to the higher income class or is able to work at home, the second group is usually in a low income class and supplies services to consumers and businesses, and is not able to provide their services in home office. In this context, the results show that the existence of these two types of social behaviours strongly affects the dynamics and possibility of a second peak in the evolution of COVID-19 in Brazil.

Based on these results, it is possible to understand that in order to master the evolution of the disease, low income people — who largely make their living on informality — must adhere to self-isolation as pointed by public health authorities worldwide. In order to solve the dilemma choosing between i) going out to get some earnings and risk being infected or ii) stay home and face starvation in favor of the latter, the present results signal it is pivotal the design of income transfer policies that pay for these people to stay at home at least 30 days after of the first peak.

Acknowledgments

The authors acknowledge financial support from the Brazilian funding agencies CNPq, CAPES and FAPERJ.

References

- [1] D. Adam, The simulations driving the worlds response to covid-19. how epidemiologists rushed to model the coronavirus pandemic?, Nature April (2020). [doi:10.1038/d41586-020-01003-6](https://doi.org/10.1038/d41586-020-01003-6).
- [2] N. Crokidakis, Covid-19 spreading in rio de janeiro, brazil: do the policies of social isolation really work?, medRxiv (2020). [doi:10.1101/2020.04.27.20081737](https://doi.org/10.1101/2020.04.27.20081737).
- [3] N. Crokidakis, Data analysis and modeling of the evolution of covid-19 in brazil, arXiv preprint arXiv:2003.12150 (2020).
- [4] S. B. Bastos, D. O. Cajueiro, Modeling and forecasting the early evolution of the covid-19 pandemic in brazil, arXiv preprint arXiv:2003.14288 (2020).
- [5] R. Li, S. Pei, B. Chen, Y. Song, T. Zhang, W. Yang, J. Shaman, Substantial undocumented infection facilitates the rapid dissemination of novel coronavirus (sars-cov-2), Science 368 (6490) (2020) 489–493. [doi:10.1126/science.abb3221](https://doi.org/10.1126/science.abb3221).
- [6] A. J. Kucharski, T. W. Russell, C. Diamond, Y. Liu, J. Edmunds, S. Funk, R. M. Eggo, Early dynamics of transmission and control of covid-19: a mathematical modelling study, The Lancet Infectious Diseases March (2020) 1–7. [doi:/10.1016/S1473-3099\(20\)30144-4](https://doi.org/10.1016/S1473-3099(20)30144-4).
- [7] D. Berger, K. Herkenhoff, S. Mongey, An seir infectious disease model with testing and conditional quarantine, Tech. rep., Federal Reserve Bank of Minneapolis (2020). [doi:10.3386/w26901](https://doi.org/10.3386/w26901).
- [8] J. M. Read, J. R. E. Bridgen, D. A. T. Cummings, A. Ho, C. P. Jewell, Novel coronavirus 2019-ncov: early estimation of epidemiological parameters and epidemic predictions, medRxiv (2020).
- [9] P. G. T. Walker, C. Whittaker, O. Watson, M. Baguelin, K. E. C. Ainslie, S. Bhatia, S. Bhatt, A. Boonyasiri, O. Boyd, L. Cattarino, Z. Cucunuba, G. Cuomo-Dannenburg, A. Dighe, C. A. Donnelly, I. Dorigatti, S. van Elsland, R. FitzJohn, S. Flaxman, H. Fu, K. Gaythorpe, L. Geidelberg, N. Grassly, W. Green, A. Hamlet, K. Hauck, D. Haw, S. Hayes, W. Hinsley, N. Imai, D. Jorgensen, E. Knock, D. Laydon, S. Mishra, G. Nedjati-Gilani, L. C. Okell, S. Riley, H. Thompson, J. Unwin, R. Verity, M. Vollmer, C. Walters, H. W. Wang, Y. Wang, P. Winskill, X. Xi, N. M. Ferguson, A. C. Ghani, The global impact of covid-19 and strategies for mitigation and suppression, Tech. rep., Imperial College (2020).

- [10] I. De Falco, A. Della Cioppa, U. Scafuri, E. Tarantino, Coronavirus covid-19 spreading in italy: optimizing an epidemiological model with dynamic social distancing through differential evolution, arXiv preprint arXiv:2004.00553 (2020).
- [11] L. Pellis, F. Scarabel, H. B. Stage, C. E. Overton, L. H. Chappell, K. A. Lythgoe, E. Fearon, E. Bennett, J. Curran-Sebastian, R. Das, et al., Challenges in control of covid-19: short doubling time and long delay to effect of interventions, arXiv preprint arXiv:2004.00117 (2020).
- [12] C. Manchein, E. L. Brugnago, R. M. da Silva, C. F. Mendes, M. W. Beims, Strong correlations between power-law growth of covid-19 in four continents and the inefficiency of soft quarantine strategies, *Chaos: An Interdisciplinary Journal of Nonlinear Science* 30 (4) (2020) 041102. doi:[10.1063/5.0009454](https://doi.org/10.1063/5.0009454).
- [13] B. F. Maier, D. Brockmann, Effective containment explains subexponential growth in recent confirmed covid-19 cases in china, *Science* 368 (6492) (2020) 742–746. doi:[10.1126/science.abb4557](https://doi.org/10.1126/science.abb4557).
- [14] G. L. Vasconcelos, A. M. Macêdo, R. Ospina, F. A. Almeida, G. C. Duarte-Filho, I. C. Souza, Modelling fatality curves of covid-19 and the effectiveness of intervention strategies, medRxiv (2020).
- [15] M. Faggian, M. Urbani, L. Zanotto, Proximity: a recipe to break the outbreak, arXiv preprint arXiv:2003.10222 (2020).
- [16] K. Muniz-Rodriguez, G. Chowell, C.-H. Cheung, D. Jia, P.-Y. Lai, Y. Lee, M. Liu, S. K. Ofori, K. M. Roosa, L. Simonsen, et al., Epidemic doubling time of the covid-19 epidemic by chinese province, medRxiv (2020).
- [17] Y. Liu, A. A. Gayle, A. Wilder-Smith, J. Rocklöv, The reproductive number of covid-19 is higher compared to sars coronavirus, *Journal of travel medicine* (2020). doi:[/10.1093/jtm/taaa021](https://doi.org/10.1093/jtm/taaa021).
- [18] S. Zhao, Q. Lin, J. Ran, S. S. Musa, G. Yang, W. Wang, Y. Lou, D. Gao, L. Yang, D. He, et al., Preliminary estimation of the basic reproduction number of novel coronavirus (2019-ncov) in china, from 2019 to 2020: A data-driven analysis in the early phase of the outbreak, *International journal of infectious diseases* 92 (2020) 214–217. doi:[10.1016/j.ijid.2020.01.050](https://doi.org/10.1016/j.ijid.2020.01.050).
- [19] A. Lai, A. Bergna, C. Acciarri, M. Galli, G. Zehender, Early phylogenetic estimate of the effective reproduction number of sars-cov-2, *Journal of medical virology* 92 (6) (2020) 675–679. doi:[10.1002/jmv.25723](https://doi.org/10.1002/jmv.25723).
- [20] N. Ferguson, D. Laydon, G. Nedjati-Gilani, N. Imai, K. Ainslie, M. Baguelin, S. Bhatia, A. Boonyasiri, Z. Cucunubá, G. Cuomo-Dannenburg, et al., Impact of non-pharmaceutical interventions (npis) to reduce covid-19 mortality and healthcare demand. imperial college covid-19 response team, Preprint at Spiral <https://doi.org/10.25561/77482> (2020).
- [21] M. U. Kraemer, C.-H. Yang, B. Gutierrez, C.-H. Wu, B. Klein, D. M. Pigott, L. du Plessis, N. R. Faria, R. Li, W. P. Hanage, et al., The effect of human mobility and control measures on the covid-19 epidemic in china, *Science* 368 (6490) (2020) 493–497. doi:[10.1126/science.abb4218](https://doi.org/10.1126/science.abb4218).
- [22] T. Zhou, Q. Liu, Z. Yang, J. Liao, K. Yang, W. Bai, X. Lu, W. Zhang, Preliminary prediction of the basic reproduction number of the wuhan novel coronavirus 2019-ncov, *Journal of Evidence-Based Medicine* 13 (1) (2020) 3–7. doi:[/10.1111/jebm.12376](https://doi.org/10.1111/jebm.12376).

- [23] M. G. Pedersen, M. Meneghini, A simple method to quantify country-specific effects of covid-19 containment measures, medRxiv (2020).
- [24] M. Bin, P. Cheung, E. Crisostomi, P. Ferraro, C. Myant, T. Parisini, R. Shorten, On fast multi-shot epidemic interventions for post lock-down mitigation: Implications for simple covid-19 models, arXiv preprint arXiv:2003.09930 (2020).
- [25] K. Biswas, A. Khaleque, P. Sen, Covid-19 spread: Reproduction of data and prediction using a sir model on euclidean network, arXiv preprint arXiv:2003.07063 (2020).
- [26] C. Tsallis, U. Tirnakli, Predicting covid-19 peaks around the world, medRxiv (2020).
- [27] T. M. Rocha Filho, F. S. G. dos Santos, V. B. Gomes, T. A. Rocha, J. H. Croda, W. M. Ramalho, W. N. Araujo, Expected impact of covid-19 outbreak in a major metropolitan area in brazil, medRxiv (2020).
- [28] A. Weber, F. Ianelli, S. Goncalves, Trend analysis of the covid-19 pandemic in china and the rest of the world, arXiv preprint arXiv:2003.09032 (2020).
- [29] P. H. P. Cintra, F. F. Nunes, Estimative of real number of infections by covid-19 on brazil and possible scenarios, medRxiv (2020).
- [30] A. Canabarro, E. Tenorio, R. Martins, L. Martins, S. Brito, R. Chaves, Data-driven study of the covid-19 pandemic via age-structured modelling and prediction of the health system failure in brazil amid diverse intervention strategies, medRxiv (2020).
- [31] A. Arenas, W. Cota, J. Gómez-Gardenes, S. Gómez, C. Granell, J. T. Matamalas, D. Soriano-Panos, B. Steinegger, A mathematical model for the spatiotemporal epidemic spreading of covid19, medRxiv (2020).
- [32] Z. Liu, Z. Deng, P. Ciais, R. Lei, S. Feng, S. J. Davis, Y. Wang, X. Yue, Y. Lei, H. Zhou, et al., Decreases in global CO_2 emissions due to covid-19 pandemic, arXiv preprint arXiv:2004.13614 (2020).
- [33] G. Bonaccorsi, F. Pierri, M. Cinelli, F. Porcelli, A. Galeazzi, A. Flori, A. L. Schmidh, C. M. Valensise, A. Scala, W. Quattrocioni, et al., Evidence of economic segregation from mobility lockdown during covid-19 epidemic, Available at SSRN 3573609 (2020).
- [34] G. Dimarco, L. Pareschi, G. Toscani, M. Zanella, Wealth distribution under the spread of infectious diseases, arXiv preprint arXiv:2004.13620 (2020).
- [35] J. Huang, H. Wang, H. Xiong, M. Fan, A. Zhuo, Y. Li, D. Dou, Quantifying the economic impact of covid-19 in mainland china using human mobility data, arXiv preprint arXiv:2005.03010 (2020).
- [36] I. L. Organization, [Women and men in the informal economy: A statistical picture](#), Tech. rep., International Labour Organization (2018).
URL https://www.ilo.org/global/publications/books/WCMS_626831/lang--en/index.htm
- [37] Z. Wang, M. A. Andrews, Z.-X. Wu, L. Wang, C. T. Bauch, Coupled disease–behavior dynamics on complex networks: A review, *Physics of life reviews* 15 (2015) 1–29. doi:10.1016/j.plrev.2015.07.006.

- [38] M. A. Pires, N. Crokidakis, Dynamics of epidemic spreading with vaccination: impact of social pressure and engagement, *Physica A* 467 (2017) 167–179. [doi:10.1016/j.physa.2016.10.004](https://doi.org/10.1016/j.physa.2016.10.004).
- [39] M. A. Pires, A. L. Oestereich, N. Crokidakis, Sudden transitions in coupled opinion and epidemic dynamics with vaccination, *J. Stat. Mech.* 2018 (5) (2018) 053407. [doi:10.1088/1742-5468/aabfc6](https://doi.org/10.1088/1742-5468/aabfc6).
- [40] N. Crokidakis, S. M. D. Queirós, Probing into the effectiveness of self-isolation policies in epidemic control, *Journal of Statistical Mechanics: Theory and Experiment* 2012 (06) (2012) P06003. [doi:10.1088/1742-5468/2012/06/P06003](https://doi.org/10.1088/1742-5468/2012/06/P06003).
- [41] M. C. Bootsma, N. M. Ferguson, The effect of public health measures on the 1918 influenza pandemic in us cities, *Proceedings of the National Academy of Sciences* 104 (18) (2007) 7588–7593. [doi:10.1073/pnas.0611071104](https://doi.org/10.1073/pnas.0611071104).
- [42] R. J. Hatchett, C. E. Mecher, M. Lipsitch, Public health interventions and epidemic intensity during the 1918 influenza pandemic, *Proceedings of the National Academy of Sciences* 104 (18) (2007) 7582–7587. [doi:10.1073/pnas.0610941104](https://doi.org/10.1073/pnas.0610941104).
- [43] L. Rogers, Ending the covid-19 epidemic in the united kingdom, arXiv preprint arXiv:2004.12462 (2020).
- [44] N. Hoertel, M. Blachier, C. Blanco, M. Olsson, M. Massetti, M. S. Rico, F. Limosin, H. Leleu, Lockdown exit strategies and risk of a second epidemic peak: a stochastic agent-based model of sars-cov-2 epidemic in france, *medRxiv* (2020).
- [45] M. G. Pedersen, M. Meneghini, Quantifying undetected covid-19 cases and effects of containment measures in italy, researchgate preprint (2020).